# The Homogeneous Master Equation and the Manipulation of Relaxation Networks[1]

**Malcolm H. Levitt[a] and Lorenzo Di Bari[b]**

[a]*Physical Chemistry Division, Arrhenius Laboratory, Stockholm University, S10691 Sweden*
[b]*Dipartimento di Chimica, via Risorgimento 35, I-56126 Pisa, Italy*

## Contents



## I. Introduction

Recently, we presented a novel method for calculating NMR spin dynamics (1). This involves a homogenous master equation (HME) and is particularly suitable for treating the interplay of incoherent relaxation processes and coherent effects such as those involving applied rf fields. The new theory provides a unified framework within which a very wide range of magnetic resonance experiments may be described. A point of special interest is the treatment of the long-term behavior of the spin system, such as the steady-state established under extensive repetition of some pulse sequence. In reference (1), we demonstrated an unusual effect: If a two-spin system is exposed to a repetitive se-

[1]Presented in part at 5th Chianti Workshop, San Miniato, Italy, May 1993.

quence of non-selective $\pi$ pulses, correlations between the nuclear spin polarizations are gradually established even where none existed before. This is manifested as a build-up of two-spin longitudinal order $< 2I_zS_z >$. The creation of two-spin order is the result of cross-correlated relaxation mechanisms, and is unconnected with the J-coupling between the spins. It runs counter to the naive expectation that a closely-spaced sequence of $\pi$ pulses should saturate the spin system (destroying all order) if applied for long enough.

In this article, we re-examine the HME and its consequences in a more physical and less formal light. We also emphasize another consequence of the HME: Carefully-chosen sequences of rf pulses may be used to simplify interconnected relaxation pathways. This is important in a number of situations (2-13): An example is the suppression of unwanted "spin diffusion" pathways in the relaxation of many-spin systems, as demonstrated by a number of groups (4,7-12). We show results here for the analogous problem of the selection of weak relaxation pathways driven by weak cross-correlation effects, in the presence of stronger autocorrelation effects. Although such experiments may also be treated within the framework of the ordinary master equation, we hope to demonstrate that the HME gives a more general and powerful insight.

## II. The Inhomogeneous Master Equation (IME)

The ordinary "master equation" for the evolution of the spin density operator $\sigma$ has the following form:

$$\frac{\mathrm{d}}{\mathrm{d}t}\sigma = -\mathrm{i}[\mathcal{H}_{\mathrm{coh}}, \sigma] + \hat{\Gamma}\,(\sigma - \sigma_{\mathrm{eq}}) \qquad (1)$$

The spin Hamiltonian $\mathcal{H}_{\mathrm{coh}}$ contains the "coherent" influences on the spin ensemble, i.e. those which are the same for all ensemble members. This includes external magnetic fields as well as the time-average of microscopic spin interactions such as chemical shifts and spin-spin couplings. The relaxation superoperator $\hat{\Gamma}$ encodes the incoherent interactions which are inhomogeneous over the spin ensemble and fluctuate in time. The master equation is valid in the "Redfield regime" of rapid fluctations (14) (assumed for the rest of this article). The elements of $\hat{\Gamma}$ can be written in terms of the spectral densities of the fluctuating incoherent interactions.

The term $\sigma_{\mathrm{eq}}$ is of particular concern. It does not appear in the unmodified Redfield theory, which uses a clean division between spin system and environment, with the states of the environment or bath implicitly uncorrelated with the nuclear spin states. As is well-known, this approximation leads to disagreement with experiment, predicting that the nuclear spin order tends to zero at long times. In fact the nuclear spin system is polarized by the contact with the environment, which has a finite temperature. The master equation is patched up by including the phenomonological correction term $\sigma_{\mathrm{eq}}$, given by (15)

$$\sigma_{\mathrm{eq}} = Z^{-1}\,\exp\{-\mathcal{H}_{\mathrm{coh}}\tau_\theta\} \qquad (2)$$

The normalization constant $Z$ is the statistical mechanical partition function and ensures $\mathrm{Tr}\{\sigma_{\mathrm{eq}}\} = 1$. The temperature $T_{\mathrm{env}}$ of the environment is denoted here by the time constant $\tau_\theta$ defined

$$\tau_\theta = \frac{\hbar}{kT_{\mathrm{env}}}\,. \qquad (3)$$

For high spin temperature $||\mathcal{H}_{\mathrm{coh}}\tau_\theta|| \ll 1$, the equilibrium density operator can be approximated

$$\sigma_{\mathrm{eq}} \cong n^{-1}\,(\hat{1} - \mathcal{H}_{\mathrm{coh}}\tau_\theta) \qquad (4)$$

where $n$ is the number of states of each individual spin system. Since $\mathcal{H}_{\mathrm{coh}}$ commutes with $\sigma_{\mathrm{eq}}$, the master equation leads to the correct convergence of $\sigma$ to $\sigma_{\mathrm{eq}}$ at long times.

The correlation of bath states with spin states leads to a shift in the equilibrium position of the spin density operator. An entirely separate issue, which will not be discussed here, is the influence of such correlations on the time-average of microscopic interactions contained in $\mathcal{H}_{\mathrm{coh}}$ (16-18).

The master equation, Eqn. 1, has a peculiar asymmetric form, with the coherent spin interactions $\mathcal{H}_{\mathrm{coh}}$ applying to the full density operator $\sigma$, while the relaxation superoperator $\hat{\Gamma}$ applies to the deviation from thermal equilibrium $\sigma - \sigma_{\mathrm{eq}}$. Mathematically, Eqn. 1 has the form of an inhomogeneous differential equation, and we will refer to it as the inhomogeneous master equation (IME).

For concreteness, we now focus on the specific system of an ensemble of heteronuclear 2-spin-1/2 pairs, each spin pair embedded in a rapidly tumbling molecule. Our main experimental case is the $^{13}$C-$^{1}$H 2-spin system of $^{13}$C-labelled liquid chloroform

($CHCl_3$). The $^1H$ spin will be denoted $I$ and the $^{13}C$ spin $S$. Each spin has a chemical shift anisotropy (CSA), and the two spins have a through-space magnetic dipole-dipole interaction (DD). Relaxation of the spin-pair system results from a combination of fluctuations in the three interactions $\mathcal{H}^{\mathrm{I}}_{\mathrm{CSA}}$, $\mathcal{H}^{\mathrm{S}}_{\mathrm{CSA}}$ and $\mathcal{H}^{\mathrm{IS}}_{\mathrm{DD}}$ (19-22). Since all have a molecular origin, all are modulated in synchrony as the molecule rotates, resulting in a finite cross-correlation between pairs of interactions (19,20,23-29). At any given time $t$, ensemble averages such as

$$\overline{\mathcal{H}^{\mathrm{IS}}_{\mathrm{DD}}(t)\mathcal{H}^{\mathrm{I}}_{\mathrm{CSA}}(t)} \tag{5}$$

do not vanish in general. The relaxation of the spin system is characterized by autocorrelation functions of the individual interactions, for example

$$\overline{\mathcal{H}^{\mathrm{IS}}_{\mathrm{DD}}(t)\mathcal{H}^{\mathrm{IS}}_{\mathrm{DD}}(0)} \tag{6}$$

and cross-correlation functions between pairs of interactions, for example

$$\overline{\mathcal{H}^{\mathrm{IS}}_{\mathrm{DD}}(t)\mathcal{H}^{\mathrm{I}}_{\mathrm{CSA}}(0)} \tag{7}$$

In the absence of applied rf fields, the IME leads to three coupled differential equations for the single-spin Zeeman polarizations $<I_z>$:

$$\frac{\mathrm{d}}{\mathrm{d}t}\begin{pmatrix} \Delta<I_z> \\ \Delta<S_z> \\ \Delta<2I_zS_z> \end{pmatrix} = \begin{pmatrix} -\rho_I & -\sigma_{IS} & -\delta_I \\ -\sigma_{IS} & -\rho_S & -\delta_S \\ -\delta_I & -\delta_S & -\rho_{IS} \end{pmatrix} \begin{pmatrix} \Delta<I_z> \\ \Delta<S_z> \\ \Delta<2I_zS_z> \end{pmatrix} \tag{8}$$

where $\Delta<\Omega>$ indicates the deviation of the expectation value of a spin operator $\Omega$ from its thermal equilibrium value:

$$\begin{aligned} \Delta<\Omega> &= <\Omega> - <\Omega>_{\mathrm{eq}} \\ &= \mathrm{Tr}\{\sigma\Omega\} - \mathrm{Tr}\{\sigma_{\mathrm{eq}}\Omega\} \ . \end{aligned} \tag{9}$$

These are known as the extended Solomon equations (20,27,29); explicit expressions for the equilibration rate constants $\rho_I$, $\rho_S$, $\rho_{IS}$, the cross-relaxation rate constant $\sigma_{IS}$, and the CSA/DD cross-correlation transfer rate constants $\delta_I$ and $\delta_S$ can be found, for example, in ref.(29).

This equation indicates a dynamic coupling of the expectation values of the three Cartesian product operators $I_z$, $S_z$ and $2I_zS_z$. The system may be pictured as three coupled "reservoirs," each containing "difference order" (deviation of the expectation value from thermal equilibrium). The difference reservoirs "leak" with rate constants $\rho_I$, $\rho_S$ and $\rho_{IS}$, and are connected by "pipes" corresponding to the cross-relaxation rate constants $\sigma_{IS}$, $\delta_I$ and $\delta_S$ (Figure 1). This picture should, however, be used cautiously: The "liquid" in each reservoir may have either sign, and the cross-relaxation rate constants may be negative, indicating that the "liquid" is changed in sign on transferring from one reservoir to another.

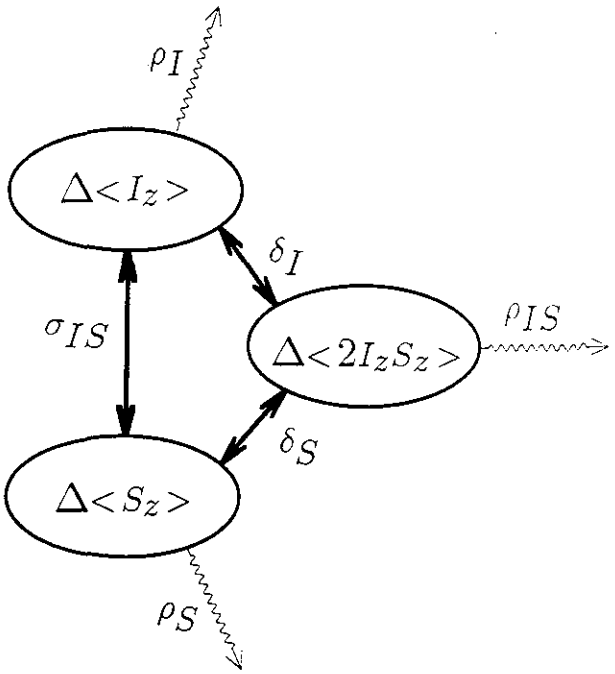


Figure 1: Physical interpretation of the extended Solomon equations for a heteronuclear 2-spin system Eqn. 8. The deviations from thermal equilibrium of the expectation values of the three spin operators form a set of coupled reservoirs.

Nevertheless, the "reservoir" picture does give a clear image of the dynamic interdependence of the three expectation values. By a careful study of the trajectories of all three expectation values after some initial perturbation, it is possible in principle to derive all the various rate constants (20). However, this is not very accurate for small rate constants, which have only a minor influence on the dynamics of the system. This problem is of course much worse for larger spin systems, where the interconnections between the expectation values are more complex still.

The measurement of small rate constants (for example, the $\delta$ terms in the above system), would be facilitated if the relaxation dynamics could be simplified, isolating selected "subnetworks." It is nat-

ural to try to accomplish this using rf pulse sequences. Analogous techniques are well-established for the simplification of spin *Hamiltonians*. For example, in decoupling experiments, large couplings between different spin species are effectively removed by applying a suitably modulated rf field to one of the species (30-33): small interactions of the non-irradiated spins are revealed even in the presence of much larger heteronuclear spin couplings. The problem of observing weak relaxation processes in the presence of stronger ones seems related.

There is, however, a theoretical difficulty in describing experiments in which rf pulses (coherent perturbations) interfere with relaxation networks (incoherent processes). In the inhomogeneous master equation, the rf fields act on the full spin density operator $\sigma$, while the relaxation applies to the difference from thermal equilibrium $\sigma - \sigma_{\rm eq}$. It is not obvious how to mix these two worlds. In the framework of the IME, it is difficult to construct an *average Liouvillian* analogous to the average Hamiltonian (30-35) so successful in treating the coherent response.

## III. The Homogeneous Master Equation (HME)

The awkward $\sigma_{\rm eq}$ term is avoided by using a homogeneous master equation (HME). This was first suggested by Jeener (36). A slightly different derivation, and some interesting applications, were sketched in (1). In this article we will concentrate on the consequences of the HME.

The rotating-frame HME (see Appendix A) has the form

$$\frac{\mathrm{d}}{\mathrm{d}t}\sigma = -\mathrm{i}[\mathcal{H}_{\rm coh}, \sigma] + \hat{\Upsilon}\sigma \ , \qquad (10)$$

where the *thermally-corrected relaxation superoperator* $\hat{\Upsilon}$ is given by

$$\hat{\Upsilon} = \hat{\Gamma} + \hat{\Theta} \ , \qquad (11)$$

and $\mathcal{H}_{\rm coh}$ is the ordinary rotating-frame Hamiltonian. Instead of including $\sigma_{\rm eq}$, the ordinary relaxation superoperator $\hat{\Gamma}$ is adjusted by adding a "thermal correction" $\hat{\Theta}$. Eqn. 10 has the mathematical form of a homogeneous first-order differential equation.

This is best illustrated by example. The HME for the relaxing 2-spin system, in the absence of rf fields, looks like

$$\frac{\mathrm{d}}{\mathrm{dt}}\begin{pmatrix} <\frac{1}{2}\mathbb{1}> \\ <I_z> \\ <S_z> \\ <2I_zS_z> \end{pmatrix} = \begin{pmatrix} 0 & 0 & 0 & 0 \\ \theta_I & -\rho_I & -\sigma_{IS} & -\delta_I \\ \theta_S & -\sigma_{IS} & -\rho_S & -\delta_S \\ \theta_{IS} & -\delta_I & -\delta_S & -\rho_{IS} \end{pmatrix} \begin{pmatrix} <\frac{1}{2}\mathbb{1}> \\ <I_z> \\ <S_z> \\ <2I_zS_z> \end{pmatrix} . \qquad (12)$$

The three new elements of the relaxation matrix are

$$\begin{aligned} \theta_I &= -\tfrac{1}{2}\left(\rho_I\omega_I^0 + \sigma_{IS}\omega_S^0\right)\tau_\theta \\ \theta_S &= -\tfrac{1}{2}\left(\sigma_{IS}\omega_I^0 + \rho_S\omega_S^0\right)\tau_\theta \\ \theta_{IS} &= -\tfrac{1}{2}\left(\delta_I\omega_I^0 + \delta_S\omega_S^0\right)\tau_\theta \ , \end{aligned} \qquad (13)$$

where $\omega_I^0$ and $\omega_S^0$ are the Larmor frequencies of the two spins.

The inclusion of the normalized unit operator $\frac{1}{2}\mathbb{1}$ has increased the dimension of the basis to 4. The expectation value $<\frac{1}{2}\mathbb{1}>$ of this operator represents the amount of *spin disorder*. The other expectation values $<I_z>$ ... are much smaller by a factor $\sim \omega_I^0\tau_\theta$ (assuming ordinary thermal nuclear spin polarization). Nevertheless, all interesting experimental observations are associated with these small quantities.

Since the top row of the new relaxation matrix contains only zeros, $<\frac{1}{2}\mathbb{1}>$ remains constant independent of the other expectation values. From Eqn. 4, the constant value is

$$<\frac{1}{2}\mathbb{1}> = \mathrm{Tr}\{\sigma_{\rm eq}\frac{1}{2}\mathbb{1}\} = \frac{1}{2} \qquad (14)$$

The dynamic independence of $<\frac{1}{2}\mathbb{1}>$ is an approximation valid for weak spin polarization. In addition, Eqn. 11 assumes a high nuclear spin temperature, and the expressions for the elements of $\hat{\Theta}$ (Eqn. 13) assume that the interaction with the static field is much larger than the other spin interactions (strong field limit). These approximations are discussed in Appendix B and are well-satisfied under ordinary circumstances.

The eigenvalues of $\hat{\Upsilon}$ are the same as $\hat{\Gamma}$, although the eigenvectors are different. This means that the thermal correction terms do not change the characteristic relaxation *rates*, only the position of the eventual equilibrium.

In Appendix B, it is shown that the elements of $\hat{\Theta}$ in Eqn. 13 may be written down by the following procedure:

1. Write down the usual Redfield relaxation matrix in a basis of Cartesian product operators (in the above case, this corresponds to the extended Solomon equations).

2. For columns corresponding to the Zeeman polarization $< I_{jz} >$ of the spin $I_j$, multiply all elements by the factor $\frac{1}{2}\omega_j^0\tau_\theta$, where $\omega_j^0$ is the Larmor frequency of spin $I_j$.

3. Multiply columns corresponding to other polarizations (such as $< 2I_{jz}I_{kz} > \ldots < I_{jx} > \ldots$) by zero.

4. Sum the elements in each row to get the corresponding element of $\hat{\Theta}$.

For example, in the current case, the second row of the Solomon matrix reads

$$\begin{array}{c} \\ <S_z> \end{array} \begin{array}{c} \begin{array}{ccc} <I_z> & <S_z> & <2I_zS_z> \end{array} \\ \begin{pmatrix} \vdots & \vdots & \vdots \\ -\sigma_{IS} & -\rho_S & -\delta_S \\ \vdots & \vdots & \vdots \end{pmatrix} \end{array} \qquad (15)$$

After multiplying by the appropriate factors, we get

$$\begin{array}{c} \\ <S_z> \end{array} \begin{array}{c} \begin{array}{ccc} <I_z> & <S_z> & <2I_zS_z> \end{array} \\ \begin{pmatrix} \vdots & \vdots & \vdots \\ -\frac{1}{2}\sigma_{IS}\omega_I^0\tau_\theta & -\frac{1}{2}\rho_S\omega_S^0\tau_\theta & 0 \\ \vdots & \vdots & \vdots \end{pmatrix} \end{array} \qquad (16)$$

Summing the row gives the correct thermal correction

$$\theta_S = -\frac{1}{2}\left(\sigma_{IS}\omega_I^0 + \rho_S\omega_S^0\right)\tau_\theta \ . \qquad (17)$$

This procedure is general for spin-1/2 systems within the approximations mentioned above.

A pictorial representation of Eqn. 12 is shown in Figure 2. The relaxation dynamics appears as a unidirectional flow from left to right in the picture. The physical significance of this "flow" is as follows: The three "reservoirs" enclosed by a dotted line contain the "spin order," which can be redistributed internally by the $\sigma$ and $\delta$ terms. The object on the left contains the large $< \frac{1}{2}\mathbb{1} >$ term, i.e. the *disorder* of the spin system. The three arrows labelled $\theta_I$, $\theta_S$ and $\theta_{IS}$ indicate the conversion of spin disorder into spin *order*, i.e. a decrease in spin entropy due to the polarizing influence of the finite-temperature molecular environment. These three terms therefore take into account the spin-bath correlations. The three wiggly arrows marked $\rho_I$, $\rho_S$ and $\rho_{IS}$ indicate the dissipation of spin order, i.e. the creation of spin entropy. These arrows do not need to "go anywhere": The destruction of order is an irreversible process which need not be balanced out somewhere else. Figure 2 is an authentic representation of the spin system as an *open system*, acting as a channel for the creation of entropy in the universe. Thermal equilibrium is established when the expectation values $< I_z >$, $< S_z >$ and $< 2I_zS_z >$ have values such that a steady flow is maintained, and as much spin entropy is created as is destroyed.

## IV. Application A: $\pi$ pulses on the I-spins

So far the HME does not appear to be much of a simplification. Its power is only revealed when relaxation and pulses are mixed together. Since the HME relaxation superoperator $\hat{\Upsilon}$ applies to the complete spin density operator, not just to the deviation from thermal equilibrium, pulse superoperators and relaxation superoperators may be combined at will. The interaction between them may be elucidated using well-known techniques.

As an example, consider a sequence of evenly-spaced strong $\pi$ pulses, separated by an interval $\tau/2$, applied to the I-spins. The relevant pulse sequence segment

$$C_A = \frac{\tau}{4} - \pi_I - \frac{\tau}{2} - \pi_I - \frac{\tau}{4} \qquad (18)$$

has total duration $\tau$.

If each $\pi$ pulse is short and ideal, it transforms the four spin operators as follows:

$$\begin{array}{rcl} \frac{1}{2}\mathbb{1} & \longrightarrow & \frac{1}{2}\mathbb{1} \\ I_z & \longrightarrow & -I_z \\ S_z & \longrightarrow & S_z \\ 2I_zS_z & \longrightarrow & -2I_zS_z \end{array} \qquad (19)$$

These equations refer to transformation properties such as

$$\exp\{-i\pi I_x\} I_z \exp\{i\pi I_x\} = -I_z \ . \qquad (20)$$

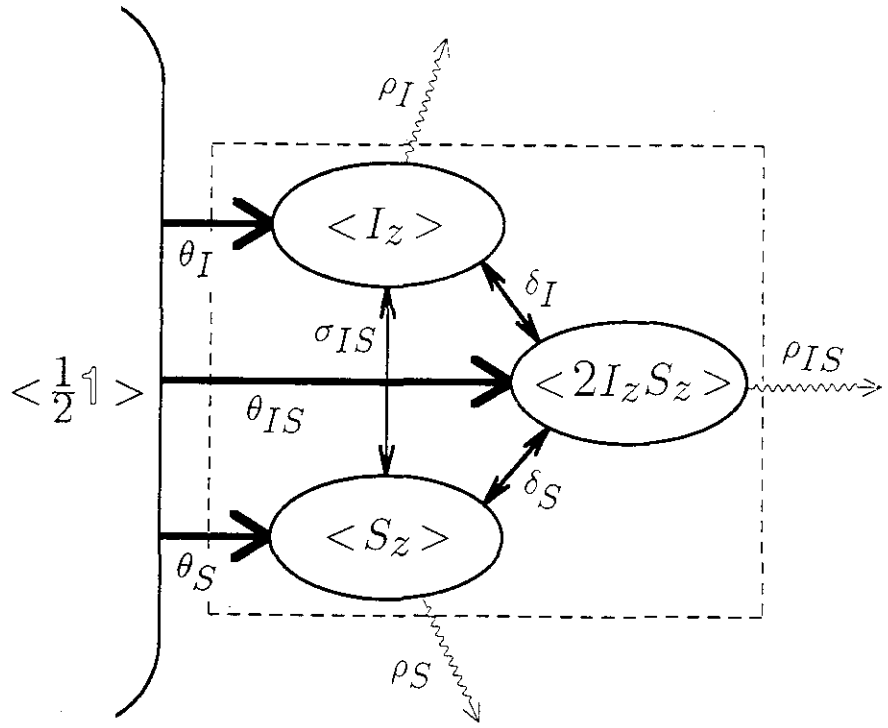


Figure 2: Physical interpretation of the HME for the 2-spin system Eqn. 12. The expectation values of the four spin operators $\frac{1}{2}\mathbb{1}$, $I_z$, $S_z$ and $2I_zS_z$ constitute reservoirs. The three terms $\theta_I$, $\theta_S$ and $\theta_{IS}$ represent the creation of spin order by polarization from the environment.

In superoperator form, the pulse can be written

$$\hat{\Pi}_I = \begin{pmatrix} 1 & & & \\ & -1 & & \\ & & 1 & \\ & & & -1 \end{pmatrix} . \tag{21}$$

The four spin operators are classified according to their *parity* under $\hat{\Pi}_I$: The two operators $\frac{1}{2}\mathbb{1}$ and $S_z$ are unchanged in sign under $\hat{\Pi}_I$, and are termed *gerade*. The two operators $I_z$ and $2I_zS_z$ are changed in sign, and are termed *ungerade*.

In the absence of rf fields, the evolution of the spin density operator from time $t_0$ to time $t_1$ is given by

$$\sigma(t_1) = \exp\{(t_1 - t_0)\,\hat{\Upsilon}\}\sigma(t_0) \tag{22}$$

It follows that the evolution of the density operator over the entire sequence $C_A$ can be written

$$\sigma(\tau + t_0) = \hat{C}_A\sigma(t_0) \tag{23}$$

where

$$\hat{C}_A = \exp\{\hat{\Upsilon}\tfrac{1}{4}\tau\}\;\hat{\Pi}_I\;\exp\{\hat{\Upsilon}\tfrac{1}{2}\tau\}\;\hat{\Pi}_I\;\exp\{\hat{\Upsilon}\tfrac{1}{4}\tau\}. \tag{24}$$

This corresponds to

$$\hat{C}_A = \exp\{\hat{\Upsilon}\tfrac{1}{4}\tau\}\exp\{\hat{\Upsilon}'\tfrac{1}{2}\tau\}\exp\{\hat{\Upsilon}\tfrac{1}{4}\tau\} \tag{25}$$

where

$$\hat{\Upsilon}' = \hat{\Pi}_I\hat{\Upsilon}\hat{\Pi}_I\ . \tag{26}$$

The matrix representation of the transformed superoperator $\hat{\Upsilon}'$ is the same as that of $\hat{\Upsilon}$, except that elements connecting operators of opposite parity are changed in sign:

$$\hat{\Upsilon}' = \begin{pmatrix} 0 & 0 & 0 & 0 \\ -\theta_I & -\rho_I & \sigma_{IS} & -\delta_I \\ \theta_S & \sigma_{IS} & -\rho_S & \delta_S \\ -\theta_{IS} & -\delta_I & \delta_S & -\rho_{IS} \end{pmatrix} . \tag{27}$$

It is convenient (but not essential) to take the limit of a cycle duration $\tau$ short compared to the relaxation time constants. An approximation to Eqn. 25 is then:

$$\hat{C}_A \cong \exp\{\frac{1}{2}\left(\hat{\Upsilon} + \hat{\Upsilon}'\right)\tau\}\ . \tag{28}$$

(This is equivalent to taking the first term in a Magnus expansion of the interaction frame Liouvillian;

by symmetry, the second term in the Magnus expansion vanishes (30-35)). The propagator for the entire sequence, including both relaxation and pulses, is therefore

$$\hat{C}_A \cong \exp\{\hat{\bar{\Upsilon}}_A \tau\} \ , \tag{29}$$

where the *effective relaxation superoperator* $\hat{\bar{\Upsilon}}_A$ has a matrix representation

$$\hat{\bar{\Upsilon}}_A = \begin{pmatrix} 0 & 0 & 0 & 0 \\ 0 & -\rho_I & 0 & -\delta_I \\ \theta_S & 0 & -\rho_S & 0 \\ 0 & -\delta_I & 0 & -\rho_{IS} \end{pmatrix} . \tag{30}$$

Thus, for rapid pulsing, the system separates dynamically into independent *gerade* and *ungerade* subspaces:

$$\hat{\bar{\Upsilon}}_A = \hat{\Upsilon}^g_A + \hat{\Upsilon}^u_A \tag{31}$$

with

$$\hat{\Upsilon}^g_A = \begin{pmatrix} 0 & 0 & 0 & 0 \\ 0 & 0 & 0 & 0 \\ \theta_S & 0 & -\rho_S & 0 \\ 0 & 0 & 0 & 0 \end{pmatrix} \tag{32}$$

and

$$\hat{\Upsilon}^u_A = \begin{pmatrix} 0 & 0 & 0 & 0 \\ 0 & -\rho_I & 0 & -\delta_I \\ 0 & 0 & 0 & 0 \\ 0 & -\delta_I & 0 & -\rho_{IS} \end{pmatrix} . \tag{33}$$

This is shown visually in Figure 3.

We now consider individually the dynamics in the two subspaces.

## 1. Dynamics in the gerade subspace

The dynamics in the gerade subspace are very simple. The expectation value $< S_z >$ is polarized at the constant rate $\theta_S < \frac{1}{2}\mathbb{1} >$ and dissipates at the rate $\rho_S < S_z >$. There is a single exponential approach to a steady-state value of S-spin polarization. If pulse cycles are $C_A$ are repeated one after the other, the value of S-spin polarization after $N$ repetitions is

$$< S_z > (N\tau) = < S_z >^{\text{ss}} + (< S_z >_0 - < S_z >^{\text{ss}}) \ \exp\{-\rho_S N\tau\} \tag{34}$$

where the initial S-spin polarization is $< S_z >_0$ and its steady-state value is

$$< S_z >^{\text{ss}} = \frac{< \frac{1}{2}\mathbb{1} > \theta_S}{\rho_S} = \frac{\theta_S}{2\rho_S} . \tag{35}$$

This evaluates to

$$\frac{< S_z >^{\text{ss}}}{< S_z >^{\text{eq}}} = 1 + \frac{\sigma_{IS}\omega^0_I}{\rho_S \omega^0_S} \tag{36}$$

using the thermal equilibrium expectation value

$$< S_z >^{\text{eq}} = \ \text{Tr}\{\sigma_{\text{eq}} S_z\} = -\frac{1}{4}\omega^0_S \tau_\theta \ . \tag{37}$$

Eqn. 36 describes the steady-state nuclear Overhauser enhancement of the S-spin magnetization on applying radio-frequency fields to the I-spin (22,37).

Although this effect is well-known, its interpretation in the HME formalism is unusual and revealing. The NOE arises because the rf fields are able to stem the leakage of S-spin polarization into the I-spin-order and two-spin-order terms. The applied fields merely turn off unwanted relaxation pathways, allowing a build-up of S-spin order under the favourable $\theta_S$ term.

## 2. Dynamics in the ungerade subspace

The dynamics in the ungerade subspace are also of interest. The central feature is that transfer of order takes place between I-spin Zeeman polarization $< I_z >$ and 2-spin order $< 2I_z S_z >$ within a dynamically simple two-dimensional subsystem. The weak cross-correlation pathway connecting the two terms is isolated, allowing a more accurate experimental measurement.

We have examined dynamic isolation of the cross-correlation pathway using the pulse sequences shown in Figure 4. The sequence in Figure 4a is used to examine the unmanipulated transfer of order from $< I_z >$ into $< S_z >$ and $< 2I_z S_z >$. Initial thermal equilibrium is disturbed by two $\pi/2$ pulses applied to the I-spins, which can have different relative phases. After a time $\tau$, a $\pi/2$ pulse is applied to the S-spins and the signal detected. Signal from experiments in which the two I-spin $\pi/2$ pulses have the same phase are subtracted from those in which the two I-spin $\pi/2$ pulses have opposite phase. As discussed in Appendix E, thermal polarization effects in the subsequent evolution may then be ignored. The contributions to $< S_z >$ and $< 2I_z S_z >$

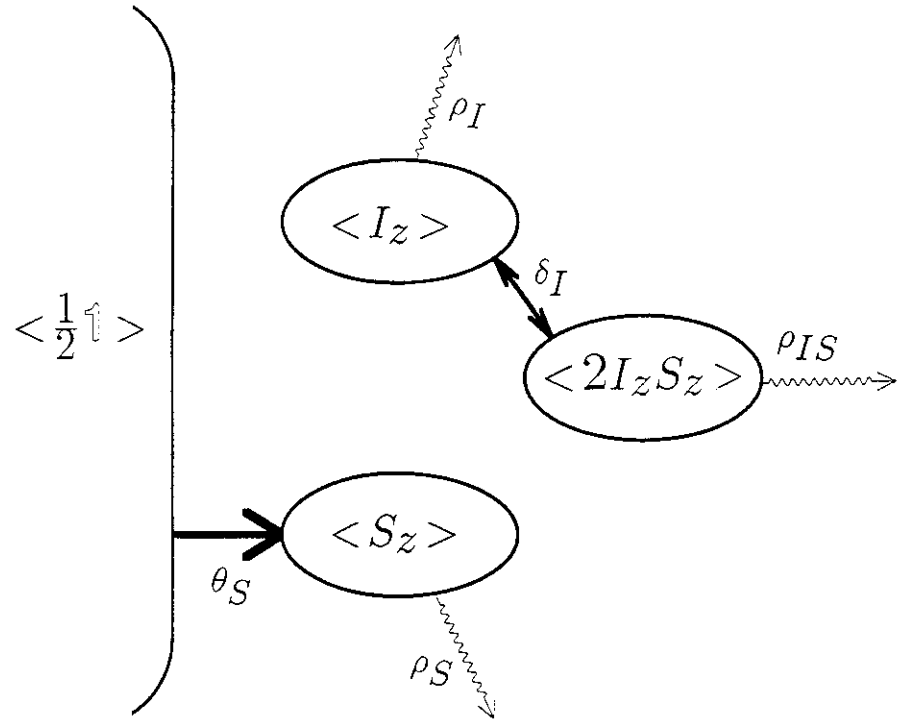


Figure 3: Relaxation dynamics in the presence of rapid $\pi$ pulses on the I-spins. The effective relaxation superoperator is factored into a *gerade* subspace $\left\{<\frac{1}{2}\mathbb{1}>, <S_z>\right\}$ and an *ungerade* subspace $\{<I_z>, <2I_zS_z>\}$.

through cross-relaxation from $< I_z >$ over the interval $\tau$ are deduced by Fourier transforming the signal and manipulating the intensities of the two lines in the J-coupled multiplet in the usual way (38,39). The experiment is repeated for a range of cross-relaxation intervals $\tau$.

The $\tau$-dependence of $< S_z >$ and $< 2I_zS_z >$ are shown in Figure 5a. The predominant process, as expected, is the rapid creation of $< S_z >$ under the dominant autocorrelation $\sigma_{IS}$ pathway. $< S_z >$ is negative since the cross-relaxation rate constant $\sigma_{IS}$ is positive for this small molecule. $< 2I_zS_z >$ is also created, but in this experiment it is not easy to tell how much of this is due to direct $<I_z>\rightarrow<2I_zS_z>$ transfer and how much to a two-step process $<I_z>\rightarrow<S_z>\rightarrow<2I_zS_z>$.

With one $\pi$ pulse on the I-spins in the middle of the mixing time (Figure 4b), the $< I_z >\rightarrow< S_z >$ transfer is greatly suppressed (Figure 5b). The $< I_z >\rightarrow< 2I_zS_z >$ transfer is also attenuated at long times, indicating the removal of two-step contributions (the change in sign on the right-hand side of Figure 5b is due to the inverting effect of the single $\pi$ pulse on the *ungerade* spin operators).

By placing two $\pi$ pulses at times $\tau/4$ and $3\tau/4$, the autocorrelation pathway $<I_z>\rightarrow<S_z>$ is eliminated and the observed polarization of $< 2I_zS_z >$ can be attributed to an essentially uncontaminated $\delta_I$ cross-correlation term. The $\tau$-dependences of $< 2I_zS_z >$ in Figure 5(b,c) are essentially mirror-images, indicating that pulse imperfections are negligible. In Figure 6 we show the difference between the $<2I_zS_z>$ curves in Figure 5a and Figure 5c on an expanded scale. This curve indicates the influence of multiple-step transfers in the unmanipulated experiment. Although in principle the derivative of the curve is zero at $\tau = 0$, the steep rise would make an "initial rate" analysis problematic.

The transfer curves could be analyzed to obtain the value $\delta_I = -1.65 \times 10^{-2}\,\mathrm{s}^{-1}$. We have strong evidence (not discussed here) that this result is more accurate than that obtained from a previous dynamical analysis of the full relaxation network, performed with the aid of two-dimensional spectroscopy (28).

## V. Application B: $\pi$ pulses on both I and S-spins

Interesting results are also obtained if the HME is used to analyze an experiment in which simulta-

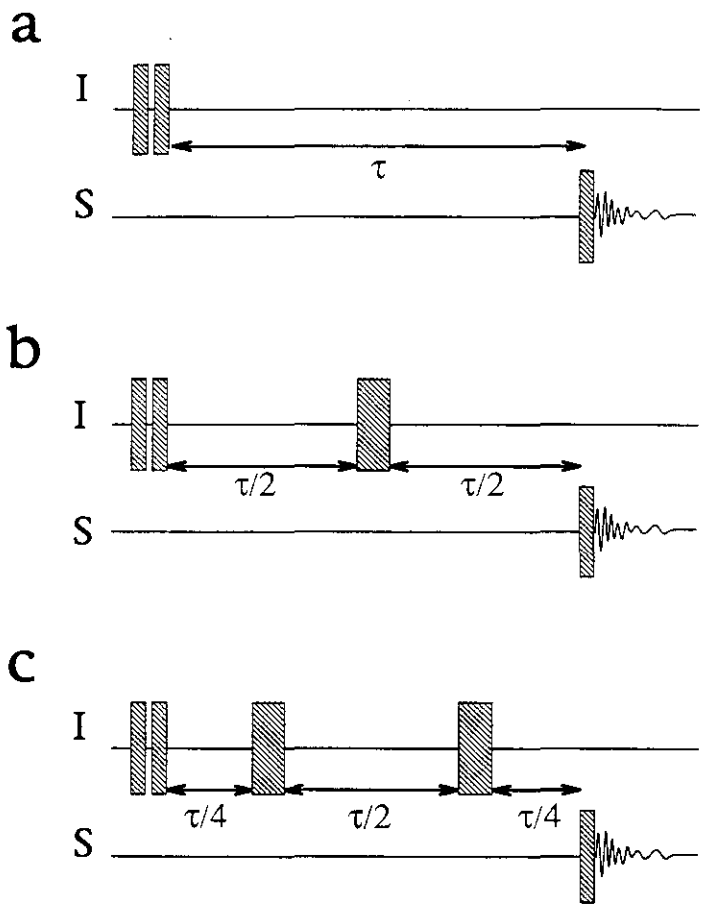


Figure 4: Pulse sequence for exploring the dynamics in the *ungerade* subspace. The experiments begin with two phase-cycled $\pi/2$ pulses on the I-spins: These select the contribution from initial $<I_z>$ polarization at the beginning of the mixing period $\tau$. A $\pi/2$ pulse on the S-spins at the end of $\tau$ and observation of the J-coupled multiplet allows detection of cross-relaxed $<S_z>$ and $<2I_zS_z>$ at the end of $\tau$. (a) No manipulations of the relaxation network. (b) One I-spin $\pi$ pulse at the centre of $\tau$ (c) Two I-spin $\pi$ pulses at $\tau/4$ and $3\tau/4$. The relative pulse lengths are greatly exaggerated with respect to the delays. In practice, composite $\pi$ pulses were used.

neous (or nearly simultaneous) $\pi$ pulses are applied to both I- and S-spin species. The relevant pulse sequence is

$$C_B = \frac{\tau}{4} - \pi_I\pi_S - \frac{\tau}{2} - \pi_I\pi_S - \frac{\tau}{4} \qquad (38)$$

which again has a total duration $\tau$.

The operators are re-classified according to their parity under the two $\pi$ rotations:

$$\begin{aligned} \tfrac{1}{2}\mathbb{1} &\longrightarrow \tfrac{1}{2}\mathbb{1} \\ I_z &\longrightarrow -I_z \\ S_z &\longrightarrow -S_z \\ 2I_zS_z &\longrightarrow 2I_zS_z \end{aligned} \qquad (39)$$

indicating transformation properties such as

$$\exp\{-\mathrm{i}\pi\,(I_x + S_x)\}2I_zS_z\,\exp\{\mathrm{i}\pi\,(I_x + S_x)\} = 2I_zS_z. \qquad (40)$$

The simultaneous $\pi$ pulse pair can therefore be represented by a rotating-frame superoperator

$$\hat{\Pi}_{IS} = \begin{pmatrix} 1 & & & \\ & -1 & & \\ & & -1 & \\ & & & 1 \end{pmatrix}. \qquad (41)$$

This time both one-spin Zeeman operators $I_z$ and $S_z$ are *ungerade*, while the two-spin-order operator $2I_zS_z$ and the normalized unit operator $\frac{1}{2}\mathbb{1}$ are *gerade*.

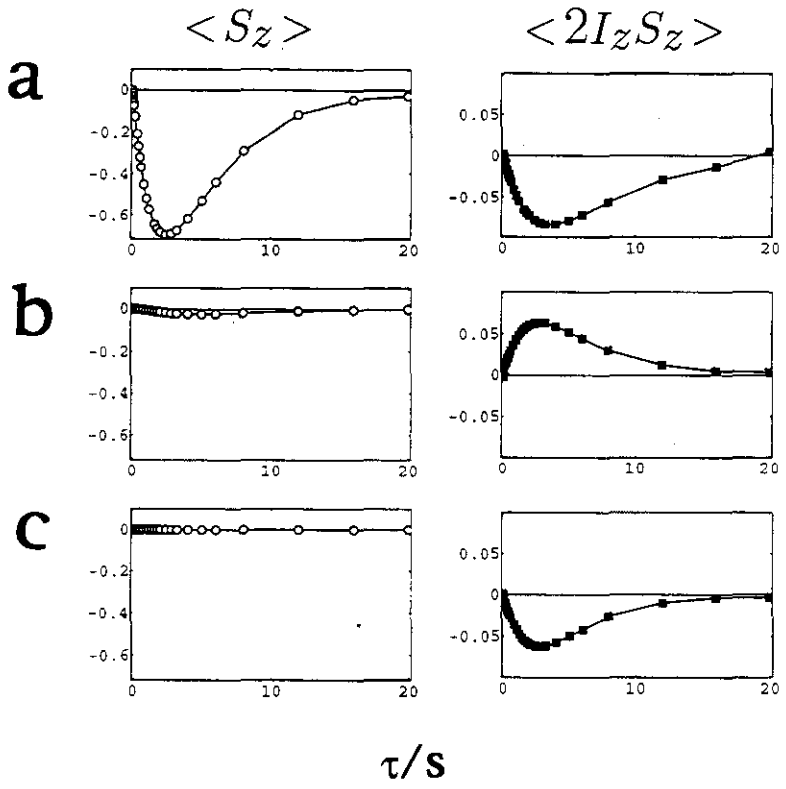


Figure 5: Experimental results for $^{13}$C-labelled chloroform at a proton frequency of 200 MHz. Rows a, b and c correspond to the experiments in Figure 4. Left column: Cross-relaxed $< S_z >$. Right column: Cross-relaxed $< 2I_zS_z >$. Vertical axes normalized to $< S_z >^{eq}$. Note the different scales. In c, the suppression of cross-relaxed $< S_z >$ indicates the isolation of the *ungerade* subspace.

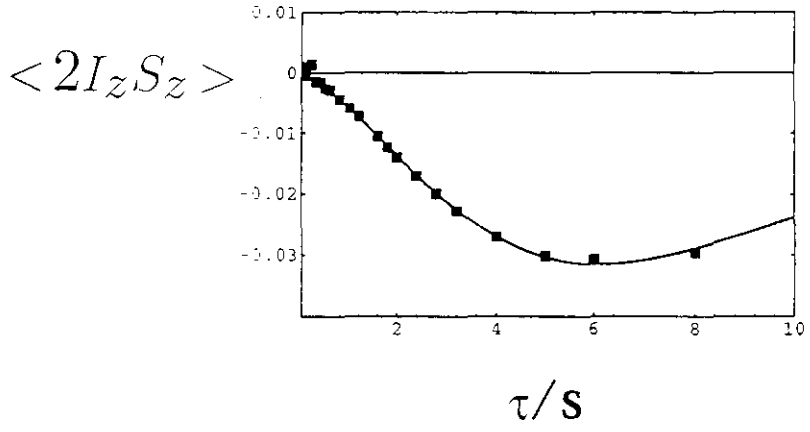


Figure 6: Difference between the $\tau$-dependences of $< 2I_zS_z >$ shown in Figure 5a and Figure 5c, on an expanded scale. The solid line has no theoretical significance. The curve has zero derivative at $\tau = 0$, but rises steeply.

If the arguments given above are repeated, we get an overall superoperator for the pulse sequence

$$\hat{C}_B \cong \exp\{\hat{\Upsilon}_B \tau\} \ , \tag{42}$$

where the effective relaxation superoperator, as modified by the rf fields, is

$$\hat{\Upsilon}_B = \hat{\Upsilon}_B^g + \hat{\Upsilon}_B^u \ . \tag{43}$$

The matrix representations of the gerade and ungerade subspace relaxation superoperators are

$$\hat{\Upsilon}_B^g = \begin{pmatrix} 0 & 0 & 0 & 0 \\ 0 & 0 & 0 & 0 \\ 0 & 0 & 0 & 0 \\ \theta_{IS} & 0 & 0 & -\rho_{IS} \end{pmatrix} \tag{44}$$

and

$$\hat{\Upsilon}_B^u = \begin{pmatrix} 0 & 0 & 0 & 0 \\ 0 & -\rho_I & -\sigma_{IS} & 0 \\ 0 & -\sigma_{IS} & -\rho_S & 0 \\ 0 & 0 & 0 & 0 \end{pmatrix} \ . \tag{45}$$

A visual representation is shown in Figure 7.

## 1. Dynamics in the ungerade subspace

The dynamics in the ungerade subspace are, as before, purely dissipative: order is transferred from $< I_z >$ to $< S_z >$ with the autocorrelation cross-relaxation rate constant $\sigma_{IS}$, accompanied by dissipation of the Zeeman orders with rate constants $\rho_I$ and $\rho_S$. This describes a normal transient nuclear Overhauser effect experiment (20), with the minor difference that the participation of cross-correlation pathways is eliminated. This experiment could therefore be used to avoid potential errors in distance estimation due to non-negligible cross-correlation effects (40,41), as demonstrated elsewhere (42). The method is analogous to the suppression of cross-correlation effects in measurements of relaxation time constants (3,43).

## 2. Dynamics in the gerade subspace

The gerade subspace in this experiment throws up a real surprise. It is naively expected that long-term irradiation by non-selective $\pi$ pulses should saturate the spin system, equalizing all populations and destroying all spin order. The HME analysis shows that on the contrary a dense sequence of non-selective $\pi$ pulses *polarizes* the multiple-spin-order terms, providing the relaxation mechanisms display suitable cross-correlation (1). By repeating the arguments used in the previous section, a steady-state of 2-spin-order can be predicted:

$$\frac{< 2I_z S_z >^{\mathrm{ss}}}{< S_z >^{\mathrm{eq}}} = \frac{\delta_I \omega_I^0 + \delta_S \omega_S^0}{\rho_{IS} \omega_S^0} \ . \tag{46}$$

It should be emphasized that the $\pi$ pulses do not merely preserve any existing two-spin order, but establish the conditions for its creation. Two-spin order develops even when the $\pi$ pulses are applied to a spin system which is totally saturated.

The effect is demonstrated by the sequence shown in Figure 8a. $N$ repetitions of the cycle $C_B$ (Eqn. 38) are applied to the $^{13}$C-$^1$H system, starting from thermal equilibrium. The total irradiation time is $T = N\tau$. Composite $\pi$ pulses $(\pi/2)_0\,(2\pi)_{2\pi/3}\,(\pi/2)_0$ were used throughout in order to reduce pulse imperfections (44). At the end of the long $\pi$ pulse train, a $\pi/2$ pulse was applied to either the I-spins or the S-spins, and the free induction decays recorded. Fourier transformation gives J-coupled doublets in the I-spin or S-spin spectra, from which the values of $< I_z > (T)$, $< S_z > (T)$ and $< 2I_z S_z > (T)$ may be extracted (20,38,39). The trajectories of the three expectation values under the $\pi$ pulse train are shown in Figure 9. As expected, the one-spin Zeeman orders $< I_z >$ and $< S_z >$ saturate under the $\pi$ pulse sequence, while negative two-spin-order grows in, eventually attaining a steady state of around $-18\%$ of the thermal equilibrium S-spin Zeeman polarization. The magnitude of the steady-state agrees quantitatively with the cross-correlation rate constants derived by the experiment in the previous section.

It is also possible to demonstrate this effect in homonuclear spin systems, using the pulse sequence shown in Figure 8b. Strong non-selective $\pi$ pulses are used, affecting all spins in the sample. At the end of the $\pi$ pulse train, a strong $\pi/4$ pulse is applied and the spectrum recorded. (A $\pi/2$ pulse would be unsuitable, since two-spin order would be completely converted into unobservable multiple-quantum coherence). The $\pi/4$ pulse partially converts two-spin Zeeman order into observable single-quantum coherence, with the lines appearing in a characteristic antiphase pattern.

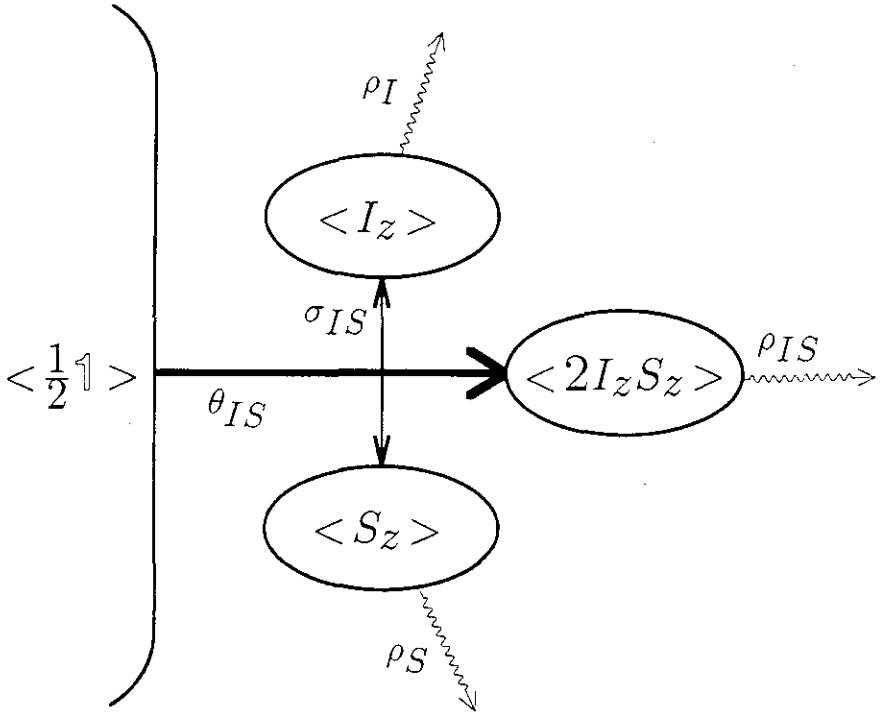


Figure 7: Relaxation dynamics in the presence of rapid $\pi$ pulses on both I and S-spins. The effective relaxation superoperator is factored into a *gerade* subspace $\left\{<\frac{1}{2}\mathbb{1}>, <2I_zS_z>\right\}$ and an *ungerade* subspace $\{<I_z>, <S_z>\}$.

Figure 10 shows a series of experimental $^1$H spectra for a sample of exifone,

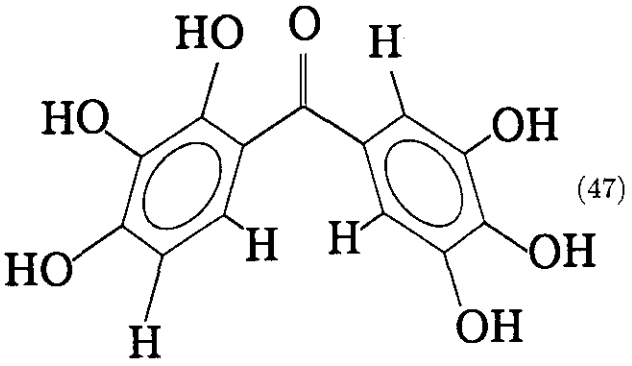


(47)

a system already used by the Lausanne group for studying cross-correlation effects (45). The normal $^1$H spectrum (lowest plot) shows a four-line AX pattern from the ortho and meta protons on one of the aromatic rings and a strong singlet from the two equivalent ortho protons on the other ring. When a long series of $\pi$ pulses is applied, the singlet gradually saturates, while the four AX lines eventually assume an antiphase character. The topmost spectrum is in the steady-state, after the application of many hundreds of $\pi$ pulses. The two-spin order is small but certainly not negligible. We report elsewhere a quantitative analysis at a set of different magnetic fields, including a treatment of pulse imperfections. These results indicate that the steady-state provides a reliable estimate of CSA-DD cross-correlation, possibly superior to the usual methods.

Burghardt et al. (46) previously observed steady-state two-spin order effects in simulations of synchronous nutation experiments (5,6) using the conventional master equation.

## VI. Discussion

In the above discussion, the HME was written implicitly in the rotating reference frame. The use of the rotating frame in the context of the HME, and spin-lattice relaxation in general, is discussed in Appendix A.

The theory of the thermal correction to the relaxation superoperator is given in Appendix B.

The above treatment was restricted to situations in which the rf fields implemented perfect, short, $\pi$ pulses. The treatment could then be restricted to a small Liouville subspace, making for a simple physical situation amenable to physical insight.

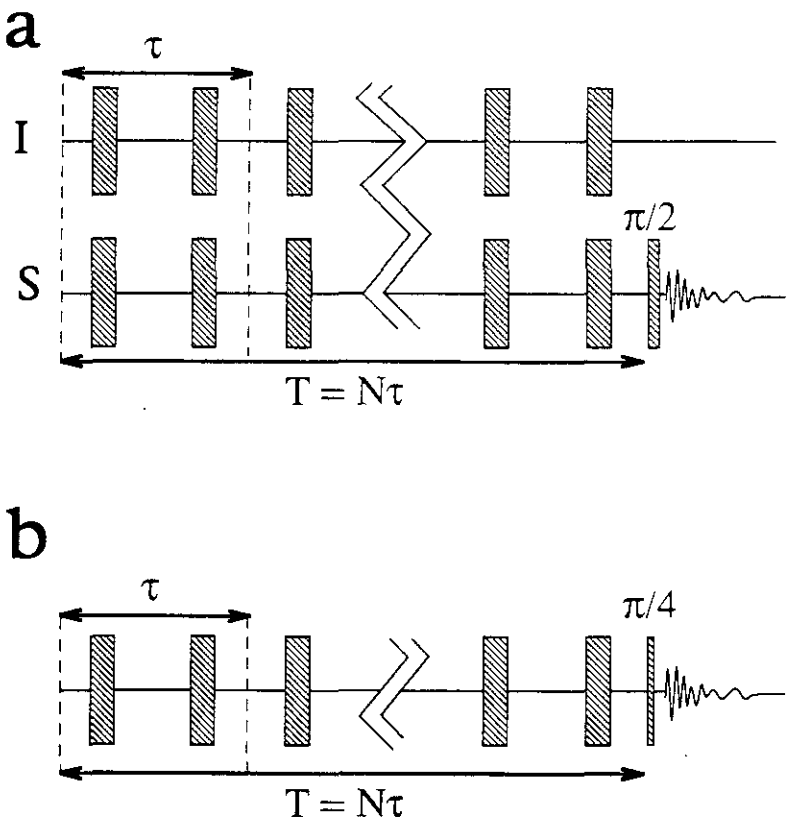


Figure 8: Pulse sequences for exploring steady-state effects in the gerade subspace; in the presence of non-selective $\pi$ pulses. (a) Heteronuclear experiment. $2N$ simultaneous $\pi$ pulses are applied over a time $T = N\tau$. A $\pi/2$ pulse on one of the spin species generates the signal. (b) Homonuclear experiment. $2N$ non-selective $\pi$ pulses are applied over a time $T = N\tau$ before a $\pi/4$ pulse is used to convert the polarizations into observable signals.

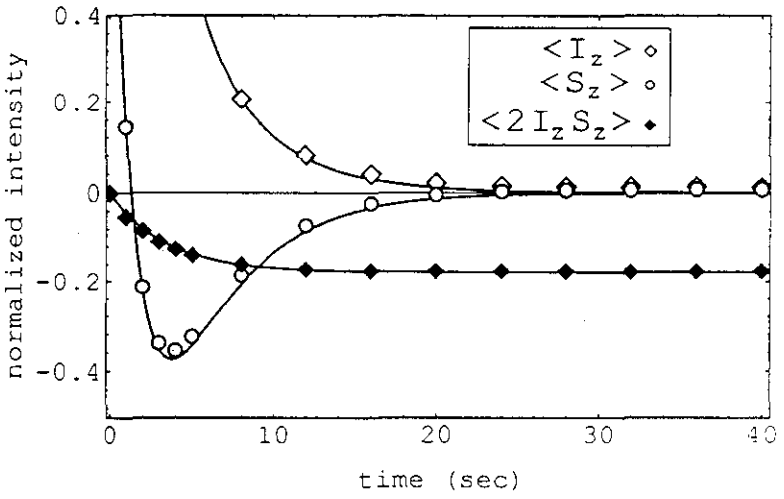


Figure 9: Experimental results for $^{13}$C-labelled chloroform at a proton frequency of 200 MHz, using the experimental sequence in Figure 8a. Composite $\pi$ pulses were actually used. The cycle period was $\tau = 200$ ms. The horizontal axis is the total irradiation time $T$. The vertical axis is normalized to $< S_z >^{eq}$. Note the build-up of $< 2I_zS_z >$.

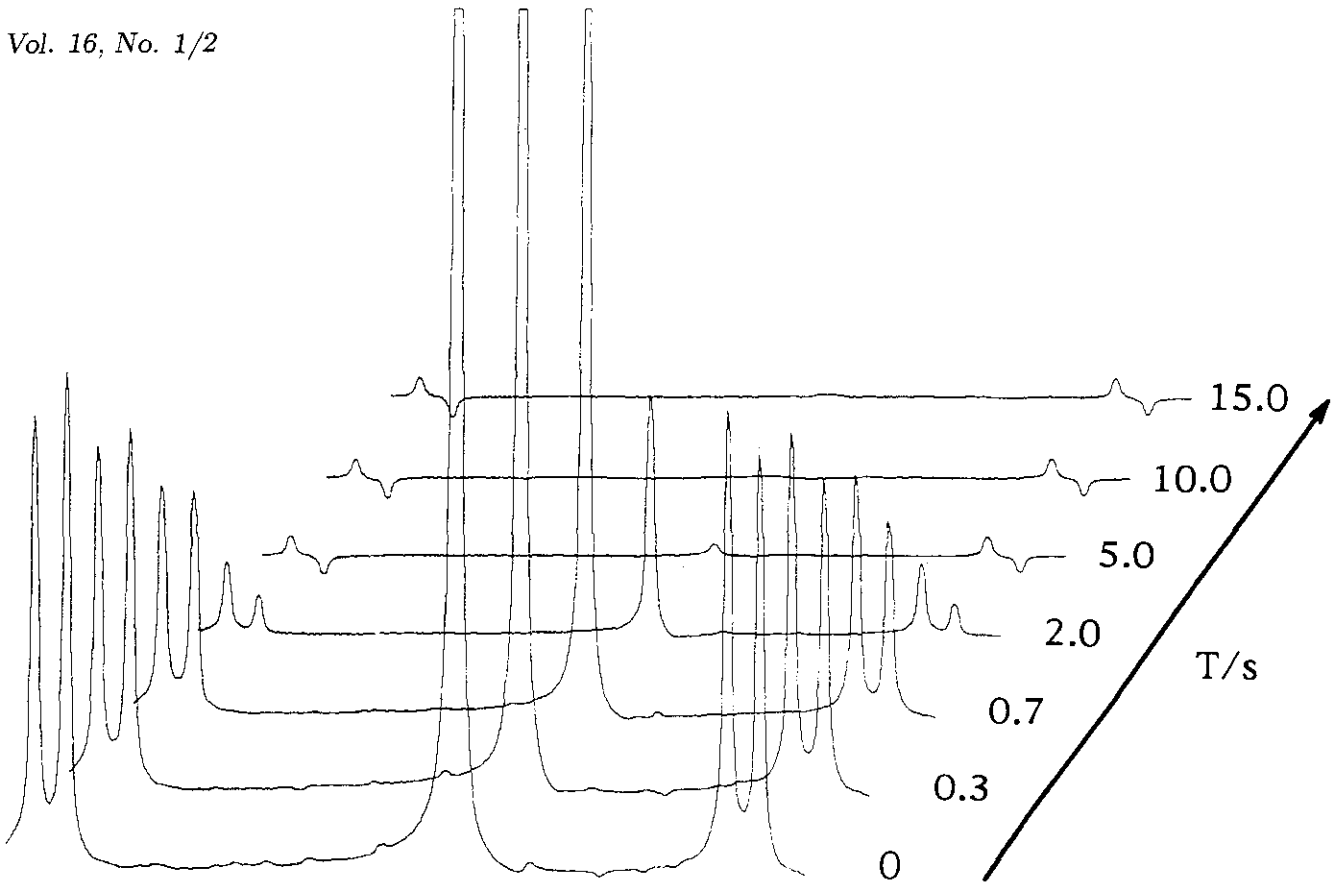


Figure 10: Experimental $^1$H spectra for exifone at a frequency of 300 MHz, using the sequence in Figure 8b. The cycle period was $\tau = 50$ ms.

Another simple case is when frequency-selective $\pi$ pulses are used. Providing the pulses operate perfectly, and relaxation during the pulse is neglected, the spin operators may be classified as *ungerade* or *gerade* with respect to the selective spin inversions. There is considerable freedom in the classification of the operators, limited only by the ease of experimental implementation on the required timescale. The interposition of selective $\pi$ pulses in the mixing period can therefore be used to restrict relaxation to an almost freely-chosen group of one-spin or multi-spin operators. For example, cross-relaxation pathways involving spins falling in a given spectral range may be *suppressed* (10), or cross-relaxation may only be *allowed* between spins falling within *two* freely-chosen spectral ranges (4,12).

Similar results may also be obtained using continuous rf fields, rather than selective $\pi$ pulses (5-8). Such experiments are also amenable to HME analysis, although a larger Liouville subspace of orthogonal spin operators must be used. This involves no particular difficulties, although calculations can become cumbersome. A simple example is given in Appendix C.

The HME is well-suited for numerical simulation (47). It provides an attractive alternative to the methods developed by Ravikumar et al. (48), who took into account thermal polarization effects in a different way. Their method involves a separate estimation of the steady-state during each element of the pulse sequence, using the conventional master equation. In contrast, HME calculations simply require the usual numerical diagonalization of the matrix representation of $\hat{\Upsilon}$. The asymmetry of the matrix representation involves no special problems. A short cut is available for periods where rf fields are absent, as discussed in Appendix D.

Griesinger et al. (49) developed a technique known as "invariant trajectories" to analyze the averaging of relaxation rates under general multiple-pulse trains. The same results follow from a straightforward HME calculation in the interaction frame, followed by the average Liouvillian approximation. Such calculations are useful for deriving "average relaxation rates" in the presence of rf fields, for example in the manipulation of spin diffusion

(4,7-12). The HME includes thermal polarization and nuclear Overhauser effects omitted from most other analyses.

Many results arising from the HME can also be derived from the conventional master equation, albeit with more trouble. For many experiments involving phase cycling or difference spectroscopy, the thermal correction term $\hat{\Theta}$ may actually be omitted, without generating incorrect results. This property is extremely important, since otherwise, a great body of NMR experiments would have to be reinterpreted. This is discussed in Appendix E.

In summary, the HME establishes a much needed link between incoherent and coherent averaging experiments. The simplification of relaxation networks may be treated on an equal footing with the simplification of spin-spin coupling networks (i.e. decoupling experiments). The extensive literature on coherent averaging (30-35) becomes directly applicable to incoherent averaging experiments. The HME provides a strong physical insight, representing the spin ensemble as an open system, exchanging energy and entropy with the surrounding molecular environment.

## VII. Acknowledgments

M.H.L. acknowledges support from the Swedish Natural Science Foundation. We would like to thank J. Kowalewski, J. Jeener, L. Mäler, A. Vega and D. Sodickson for communications, help and discussions. We would also like to thank I. Burghardt for a copy of her doctoral thesis, and G. Bodenhausen for discussions and the sample of Exifone.

## VIII. Appendix A: The HME in the rotating frame

The HME is normally used in the rotating frame, where the dynamics under radio-frequency fields appear particularly simple. However, there is scope for confusion as to the correct expression for the relaxation equations in the rotating frame, and numerous errors in the literature can be found. The problem is that the spin system exchanges energy with the lattice, which is indifferent to the rotating frame used to analyze the spins. The comment of Abragam may be recalled (15): "spin and lattice temperatures are defined in two different frames of reference and there is danger of being led astray by intuitive physical arguments in this unfamiliar situation."

The main problems center around the use of the term "rotating-frame Hamiltonian," i.e. the operator which generates the spin dynamics, as corrected for illusory forces arising from the motion of the frame (50). For example the equation of motion (neglecting relaxation) of a rotating-frame spin density operator defined by

$$\sigma^R(t) = \exp\{\mathrm{i}\omega t I_z\}\ \sigma(t)\ \exp\{-\mathrm{i}\omega t I_z\} \qquad (48)$$

is

$$\frac{\mathrm{d}}{\mathrm{d}t}\sigma^R = -\mathrm{i}[\mathcal{H}^R_{\mathrm{coh}}, \sigma^R] \qquad (49)$$

with the "rotating-frame Hamiltonian"

$$\mathcal{H}^R_{\mathrm{coh}} = \exp\{\mathrm{i}\omega t I_z\}\ \mathcal{H}_{\mathrm{coh}}\ \exp\{-\mathrm{i}\omega t I_z\} - \omega I_z\ . \qquad (50)$$

This type of "rotating-frame Hamiltonian" is so familiar in NMR theory that it is often forgotten that it is not a real Hamiltonian at all. It is a sort of "pseudo-Hamiltonian" which fulfils the dynamic but not the energetic function of a true Hamiltonian. In particular, $<\mathcal{H}^R_{\mathrm{coh}}>$ is not the energy of the spin system (51), and $\mathcal{H}^R_{\mathrm{coh}}$ cannot be used in statistical thermodynamical expressions involving the spin system energy. For example, the steady-state density operator in the presence of a field has *no relationship* with the "rotating-frame Hamiltonian":

$$\sigma^R_{\mathrm{ss}} \neq Z^{-1} \exp\{-\mathcal{H}^R_{\mathrm{coh}}\tau_\theta\}\ . \qquad (51)$$

Erroneous statements to the contrary can unfortunately be found in many textbooks and papers.

A false impression is also left by the unfortunate terminology "spin-lattice relaxation in the rotating frame" and "rotating-frame nuclear Overhauser effect." These phenomena involve relaxation dynamics in the presence of rf fields, and have no particular connection with the use of a rotating frame.

To elucidate the role of the rotating frame, consider the (lab frame!) HME in the presence of an applied rf field:

$$\frac{\mathrm{d}}{\mathrm{d}t}\sigma(t) = \left(-\mathrm{i}\hat{\mathcal{H}}_{\mathrm{coh}}(t) + \hat{\Upsilon}(t)\right)\sigma(t)\ , \qquad (52)$$

where $\hat{\mathcal{H}}_{\mathrm{coh}}$ is the commutation superoperator with the time-dependent coherent Hamiltonian

$$\hat{\mathcal{H}}_{\mathrm{coh}}\Omega = [\mathcal{H}_{\mathrm{coh}}, \Omega]\ , \qquad (53)$$

and the coherent Hamiltonian is assumed to have a large, time-independent, component $\mathcal{H}_0$ and a small, time-dependent component $\mathcal{H}_1$:

$$\mathcal{H}_{\text{coh}} = \mathcal{H}_0 + \mathcal{H}_1(t) \tag{54}$$

In principle, the relaxation superoperator is also time-dependent, since the eigenstates and energies of the spin system are affected by the modulation of $\mathcal{H}_{\text{coh}}$. However, if $\mathcal{H}_1$ is much smaller than $\mathcal{H}_0$, and the fluctuations in the incoherent interactions are rapid compared to the magnitude of $\mathcal{H}_1$, the effect of $\mathcal{H}_1$ on $\hat{\Upsilon}$ may be ignored and the HME approximated as

$$\frac{\mathrm{d}}{\mathrm{d}t}\sigma(t) \cong \left(-\mathrm{i}\hat{\mathcal{H}}_{\text{coh}}(t) + \hat{\Upsilon}_0\right)\sigma(t) \ , \tag{55}$$

where $\hat{\Upsilon}_0$ is the relaxation superoperator in the absence of the rf field.

By using a transformed density operator of the form Eqn. 48, the HME becomes

$$\frac{\mathrm{d}}{\mathrm{d}t}\sigma^R(t) \cong \left(-\mathrm{i}\hat{\mathcal{H}}^R_{\text{coh}} + \hat{\Upsilon}_0\right)\sigma^R(t) \ , \tag{56}$$

where, for a proper choice of frame, the "pseudo-Hamiltonian" $\mathcal{H}^R_{\text{coh}}$ in Eqn. 50 can be made time-independent. This is the most useful form of the HME: Normally the rotating-frame is assumed and the superscripts "R" and subscript "0" dropped.

# IX. Appendix B: The thermal correction $\hat{\Theta}$

Since the lattice has a finite temperature, the probability of the nuclear spin system making a transition $|r> \rightarrow |s>$ differs slightly from that for the reverse transition $|s> \rightarrow |r>$ according to the relative energy of the two states. Elementary considerations of this kind lead to an "improved" relaxation superoperator of the form

$$\hat{\Upsilon} = \hat{\Gamma}\,\exp\{\hat{\omega}\tau_\theta\} \tag{57}$$

where the superoperator $\hat{\omega}$ has the property

$$\hat{\omega}\Omega = \sum_r \omega_r \Omega_{rr} |r><r| \ . \tag{58}$$

The sum is over all eigenstates $|r>$ of the main part of the coherent (lab frame!) Hamiltonian

$$\mathcal{H}_0|r> = \omega_r|r> \ . \tag{59}$$

Thus $\hat{\omega}$ projects out the "secular" components of an operator $\Omega$, weighting each component with the energy of the corresponding spin state.

For high nuclear spin temperature, the exponential in Eqn. 57 can be approximated by the first two terms in a series, giving

$$\hat{\Upsilon} \cong \hat{\Gamma} + \hat{\Theta} \tag{60}$$

with

$$\hat{\Theta} = \hat{\Gamma}\hat{\omega}\tau_\theta \ . \tag{61}$$

This looks simple but gives rise to rather complicated expressions.

Consider therefore the projection superoperator $\hat{P}_{\mathbb{1}}$ which removes all traceless components of its argument operator:

$$\hat{P}_{\mathbb{1}}\Omega = n^{-1}\,\mathrm{Tr}\{\Omega\}\,\mathbb{1} \ . \tag{62}$$

This can be used to decompose the density operator into a non-traceless and a traceless component:

$$\sigma = \hat{P}_{\mathbb{1}}\sigma + \left(\hat{1} - \hat{P}_{\mathbb{1}}\right)\sigma \ . \tag{63}$$

The HME can therefore be written

$$\begin{aligned}\frac{\mathrm{d}}{\mathrm{d}t}\sigma = &\left(-\mathrm{i}\hat{\mathcal{H}}_{\text{coh}} + \hat{\Gamma}\right)\sigma + \hat{\Gamma}\hat{\omega}\hat{P}_{\mathbb{1}}\sigma\tau_\theta \\ &+ \hat{\Gamma}\hat{\omega}\left(\hat{1} - \hat{P}_{\mathbb{1}}\right)\sigma\tau_\theta .\end{aligned} \tag{64}$$

Since the traceless part of the density operator is much smaller than the non-traceless part, by a factor of the order of $||\hat{\omega}\tau_\theta||$, the last term is proportional to $||\hat{\omega}\tau_\theta||^2$ and can be ignored. The thermal correction is

$$\hat{\Theta} \cong \hat{\Gamma}\hat{\omega}\hat{P}_{\mathbb{1}}\tau_\theta \tag{65}$$

which proves easier to handle.

An expression for the elements of $\hat{\Theta}$ in a base of normalized Cartesian product operators (38,39) can be derived as follows: Consider a spin system with $n$ eigenstates. A suitable set of product operators is defined by $\{Q_1, Q_2 \ldots\} = 2n^{-1/2}\left\{\frac{1}{2}\mathbb{1}, I_{1z}, I_{2z} \ldots 2I_{1z}I_{2z} \ldots\right\}$. The operators are normalized such that

$$\mathrm{Tr}\{Q_j Q_k\} = \delta_{jk} \ . \tag{66}$$

Now all elements $\theta_{jk} = \mathrm{Tr}\{Q_j\hat{\Theta}Q_k\}$ with $k \neq 1$ vanish since $Q_{k>1}$ are traceless. Similarly, all elements

$\theta_{1k}$ vanish since $\hat{\Gamma}$ is symmetrical and $\hat{\Gamma}\mathbb{1} = 0$. We are left with the elements in the first column, $\theta_{j1}$ with $j \neq 1$. These may be written as follows:

$$\theta_{j1} = \mathrm{Tr}\{Q_j \hat{\Gamma} \hat{\omega} \hat{P}_{\mathbb{1}} Q_1\} \tau_\theta \ . \tag{67}$$

Since $\hat{P}_{\mathbb{1}} Q_1 = Q_1$, this becomes

$$\theta_{j1} = \mathrm{Tr}\{Q_j \hat{\Gamma} \hat{\omega} Q_1\} \tau_\theta \ . \tag{68}$$

Using the definition of $\hat{\omega}$, and $Q_1 = n^{-1/2}\mathbb{1}$, we get

$$\theta_{j1} = n^{-1/2} \sum_{rk} \omega_r \tau_\theta \Gamma_{jk} < r|Q_k|r > \ , \tag{69}$$

introducing the elements of the ordinary relaxation matrix in the Cartesian product basis

$$\Gamma_{jk} = \mathrm{Tr}\{Q_j \hat{\Gamma} Q_k\} \ , \tag{70}$$

and the matrix elements $< r|Q_k|r >$ of spin operators $Q_k$, in the eigenbase of the coherent Hamiltonian. Now in high field, the energies $\omega_r$ are very close to the eigenvalues of the pure Zeeman Hamiltonian defined by

$$\mathcal{H}_Z^0 = \sum_\mu \omega_\mu^0 I_{\mu z} \ , \tag{71}$$

where $\omega_\mu^0$ is the Larmor frequency of spin $I_\mu$, ignoring chemical shifts and spin-spin couplings. Hence the thermal correction elements can be written

$$\theta_{j1} = n^{-1/2} \sum_{rk} \Gamma_{jk} < r|Q_k|r >< r|\mathcal{H}_Z^0|r > \tau_\theta \ . \tag{72}$$

Since $\mathcal{H}_Z^0$ is diagonal for a spin system in high field (this is true even for strongly-coupled systems), this can be written in turn

$$\theta_{j1} = n^{-1/2} \sum_k \Gamma_{jk} \ \mathrm{Tr}\{Q_k \mathcal{H}_Z^0\} \tau_\theta \ , \tag{73}$$

or more explicitly

$$\theta_{j1} = n^{-1/2} \sum_{\mu k} \omega_\mu^0 \tau_\theta \Gamma_{jk} \ \mathrm{Tr}\{Q_k I_{\mu z}\} \ . \tag{74}$$

Since for spins-1/2, $\mathrm{Tr}\{I_{\mu z}^2\} = n/4$, this equation encodes the simple step-by-step procedure given in the text for the thermal correction elements (Eqns. 15-17).

# X. Appendix C: Continuous rf fields

We give one example of the HME in a situation where additional operators must be included in the relevant Liouville subspace. Consider a heteronuclear two-spin system with continuous, on-resonance rf irradiation of the S-spin. This has been treated by Boulat and Bodenhausen (52) who showed that a naive application of the Solomon equations for the spin state populations fails. It is necessary to take into account the full spin dynamics, including the creation of spin coherences by the rf field.

The rotating-frame HME in the presence of the rf field is

$$\frac{\mathrm{d}}{\mathrm{dt}} \begin{pmatrix} <\frac{1}{2}\mathbb{1}> \\ <I_z> \\ <S_z> \\ <S_x> \end{pmatrix} = \begin{pmatrix} 0 & 0 & 0 & 0 \\ \theta_I & -\rho_I & -\sigma_{IS} & 0 \\ \theta_S & -\sigma_{IS} & -\rho_S & -\omega_1 \\ 0 & 0 & \omega_1 & -\rho_S^t \end{pmatrix} \begin{pmatrix} <\frac{1}{2}\mathbb{1}> \\ <I_z> \\ <S_z> \\ <S_x> \end{pmatrix} \tag{75}$$

where $\rho_S^t$ is the transverse relaxation rate constant of S-spin coherences, and cross-correlation effects are neglected this time. The rf field is considered to have magnitude $\omega_1$ in frequency units and phase $\pi/2$. The Liouville subspace is extended by one row and one column, in order to encompass the mixing of the rotating-frame expectation values $< S_z >$ and $< S_x >$ by the rf field.

Eqn. 75 contains the full dynamical behaviour of the system, which could in principle be extracted by diagonalizing the $4 \times 4$ matrix $\boldsymbol{A}$ in the equation above. Let us just concentrate on the steady-state behaviour. The steady-state expectation values of the spin system form a vector $\boldsymbol{v}_{\mathrm{ss}}$ which lies in the *nullspace* of $\boldsymbol{A}$ i.e.

$$\boldsymbol{A}\boldsymbol{v}_{\mathrm{ss}} = \boldsymbol{0} \ . \tag{76}$$

The nullspace is the set of eigenvectors with zero eigenvalue (53).

In the present case, the actual steady state is that nullspace vector with $<\frac{1}{2}\mathbb{1}> = \frac{1}{2}$. Explicit calculation, or computer algebra (54) gives the result immediately:

$$\begin{pmatrix} <\frac{1}{2}\mathbb{1}> \\ <Iz>^{\mathrm{ss}} \\ <Sz>^{\mathrm{ss}} \\ <Sx>^{\mathrm{ss}} \end{pmatrix} = \begin{pmatrix} \frac{1}{2} \\ X\left(\Delta^2 \rho_S^t \omega_I^0 \tau_\theta + \left(\rho_I \omega_I^0 + \sigma_{IS} \omega_S^0\right) \omega_1^2 \tau_\theta\right) \\ X\left(\Delta^2 \rho_S^t \omega_S^0 \tau_\theta\right) \\ X\left(\Delta^2 \omega_1 \omega_S^0 \tau_\theta\right) \end{pmatrix} \tag{77}$$

where

$$\Delta^2 = \rho_I \rho_S - \sigma_{IS}^2 \tag{78}$$

and

$$X = -\frac{1}{4}\left(\Delta^2 \rho_S^t + \rho_I \omega_1^2\right)^{-1} . \tag{79}$$

In the limit of $\omega_1$ much greater than the relaxation rates, and neglecting second-order effects, the expression reduces to

$$\begin{pmatrix} <\frac{1}{2}\mathbb{1}> \\ <Iz>^{ss} \\ <Sz>^{ss} \\ <Sx>^{ss} \end{pmatrix} \cong \begin{pmatrix} \frac{1}{2} \\ -\left(4\rho_I\right)^{-1}\left(\rho_I \omega_I^0 + \sigma_{IS}\omega_S^0\right)\tau_\theta \\ 0 \\ -\left(4\rho_I\omega_1\right)^{-1}\Delta^2 \omega_S^0 \tau_\theta \end{pmatrix} \tag{80}$$

Since the thermal equilibrium value of S-spin Zeeman polarization is given by

$$<S_z>^{eq} = -\frac{1}{4}\omega_S^0 \tau_\theta \tag{81}$$

the steady-state value of the *transverse* S-spin polarization $<S_x>$ in the presence of the rf field is

$$\frac{<S_x>^{ss}}{<S_z>^{eq}} \cong \frac{\Delta^2}{\rho_I \omega_1} , \tag{82}$$

and the steady-state nuclear Overhauser enhancement of the longitudinal I-spin polarization is described by

$$\frac{<I_z>^{ss}}{<I_z>^{eq}} \cong 1 + \frac{\sigma_{IS}\omega_S^0}{\rho_I \omega_I^0} , \tag{83}$$

i.e. the same as when $\pi$ pulses are used. These results are in agreement with the calculation by Boulat and Bodenhausen (52).

# XI. Appendix D: Numerical calculations with the HME

The HME may be used for numerical spin-dynamical calculations involving simultaneous relaxation and rf fields. In general, this can be done one pulse sequence element at a time. The evolution superoperator under a pulse sequence element $B$ has the form

$$\hat{B} = \exp\{\left(\hat{\mathcal{L}} + \hat{\Theta}\right)\tau\} \tag{84}$$

where $\tau$ is the pulse sequence element duration and $\hat{\mathcal{L}}$ is the effect of rf fields and relaxation, without the thermal correction:

$$\hat{\mathcal{L}} = -\mathrm{i}\hat{\mathcal{H}}_{\mathrm{coh}} + \hat{\Gamma} . \tag{85}$$

The exponential in Eqn. 84 can be calculated numerically in the usual way, by forming a matrix representation of the superoperator and diagonalizing. The asymmetry of the matrix representation generates no particular problems.

We point out here a special feature of Eqn. 84. Since $\hat{\mathcal{L}}\mathbb{1} = 0$, we have $\hat{\Theta}\hat{\mathcal{L}} = \hat{\Theta}^2 = \hat{0}$. Hence

$$\begin{aligned} \left(\hat{\mathcal{L}} + \hat{\Theta}\right)^2 &= \hat{\mathcal{L}}^2 + \hat{\mathcal{L}}\hat{\Theta} \\ \left(\hat{\mathcal{L}} + \hat{\Theta}\right)^3 &= \hat{\mathcal{L}}^3 + \hat{\mathcal{L}}^2\hat{\Theta} , \end{aligned} \tag{86}$$

and so on. It follows that the exponent can be written

$$\exp\{\left(\hat{\mathcal{L}} + \hat{\Theta}\right)\tau\} = \exp\{\hat{\mathcal{L}}\tau\} + \sum_n^\infty \frac{\hat{\mathcal{L}}^n}{(n+1)!}\hat{\Theta} \tag{87}$$

The evolution superoperator is itself the sum of a "normal" superoperator and a thermal correction term. This has important consequences (see Appendix E). Furthermore, in the special case of "free precession periods" where no rf fields are applied, Eqn. 87 may be set in the form

$$\exp\{\left(\hat{\mathcal{L}}_0 + \hat{\Theta}\right)\tau\} = \exp\{\hat{\mathcal{L}}_0\tau\} + \left(\exp\{\hat{\mathcal{L}}_0\tau\} - \mathbb{1}\right)\hat{\omega}\hat{P}_{\mathbb{1}}\tau_\theta \tag{88}$$

For free precession, the thermally corrected evolution superoperator may be derived from the non-thermally corrected superoperator, in just the same way as $\hat{\Upsilon}$ can be derived from $\hat{\Gamma}$.

# XII. Appendix E: The HME and phase cycling

Many magnetic resonance experiments involve taking a linear combination of results from related but slightly different experiments. A typical example is phase cycling, in which the experiments only differ in the relative phase of some of the pulses. The signals from the phase-shifted experiments are multiplied by complex phase factors and combined in the processing device.

For many experiments of this kind the thermal correction terms $\hat{\Theta}$ may be omitted from at least part of the calculation. This is fortunate, since it has been common practice to disregard the thermal polarization effects when convenient. A formal justification in the context of the HME may be useful.

In the treatment by Ernst and co-workers (38), phase cycling is represented by an instantaneous projection of the density operator onto a subspace of operators with particular rotational properties, i.e. coherences of particular orders. This is very convenient for calculations. All elements of the density operator which do not belong to coherences of a given order are simply removed and the calculation carried further using only the elements which do have the "right" order.

The basis for this procedure is awkward in terms of the ordinary master equation since the $\sigma_{eq}$ terms get in the way (55). It also not obvious what happens in the case of extended rf fields. In the HME, the treatment of phase cycling is more straightforward. Suppose a pulse sequence consists of two parts, $A$ and $B$. The $B$ part is performed in two versions, $B_1$ and $B_2$, and the NMR signals $s_1$ and $s_2$ combined with complex factors $c_1$ and $c_2$. In the HME, the individual NMR signals can be written

$$\begin{aligned} s_1(t) &= \mathrm{Tr}\{\Omega^+ \exp\{\hat{\mathcal{L}}_0 t\}\hat{B}_1\hat{A}\sigma_0\} \\ s_2(t) &= \mathrm{Tr}\{\Omega^+ \exp\{\hat{\mathcal{L}}_0 t\}\hat{B}_2\hat{A}\sigma_0\} \ , \end{aligned} \quad (89)$$

where $\Omega$ is the observable operator and $\sigma_0$ the initial density operator, assumed identical in the two experiments. The combined signal $c_1 s_1(t) + c_2 s_2(t)$ can be written

$$\overline{s(t)} = \mathrm{Tr}\{\Omega^+ \exp\{\hat{\mathcal{L}}_0 t\}\overline{\hat{B}}\hat{A}\sigma_0\} \quad (90)$$

where

$$\overline{\hat{B}} = c_1\hat{B}_1 + c_2\hat{B}_2 \ . \quad (91)$$

Thus the superoperators of different pulse sequences are combined linearly. In phase cycling, the experiments are selected such that the averaged superoperator behaves according to:

$$\overline{\hat{B}} = \hat{B}\hat{P}_M \quad (92)$$

where $\hat{P}_M$ projects out operator terms belonging to spin coherences of a particular order $M$, or set of orders.

From Eqn. 87, the superoperator including phase cycling, for $M \neq 0$, is

$$\exp\{\left(\hat{\mathcal{L}} + \hat{\Theta}\right)\tau\}\hat{P}_M = \exp\{\hat{\mathcal{L}}\tau\}\hat{P}_M \ . \quad (93)$$

The "thermal correction" vanishes since $\hat{P}_1\hat{P}_M = \hat{0}$.

It follows that if phase cycling is used to select coherences of some *non-zero* order $M$ at a particular point in a pulse sequence, the thermal correction terms may safely be omitted from all *subsequent* pulse sequence elements. Similar conclusions apply to other forms of difference spectroscopy.

## XIII. References


[1]M. H. Levitt and L. Di Bari, *Phys. Rev. Lett.* **69**, 3124 (1992).

[2]T. E. Bull, *J. Magn. Reson.* **93**, 596 (1991).

[3]L. E. Kay, L. K. Nicholson, F. Delaglio, A. Bax and D. A. Torchia, *J. Magn. Reson.* **97**, 359 (1992).

[4]G. Bodenhausen, 5th Chianti Workshop, San Miniato, Italy, May 1993.

[5]B. Boulat, I. Burghardt and G. Bodenhausen, *J. Am. Chem. Soc.* **114**, 10679 (1992).

[6]I. Burghardt, R. Konrat, B. Boulat, S. J. F. Vincent and G. Bodenhausen, *J. Chem. Phys.* **98**, 1721 (1993).

[7]E. T. Olejniczak, R. T. Gampe and S. W. Fesik, *J. Magn. Reson.* **67**, 28 (1986).

[8]W. Massefski and A. G. Redfield, *J. Magn. Reson.* **78**, 150 (1988).

[9]J. Fejzo, W. M. Westler, S. Macura and J. L. Markley, *J. Magn. Reson.* **92**, 20 (1991).

[10]J. Fejzo, W. M. Westler, S. Macura and J. L. Markley, *J. Magn. Reson.* **92**, 195 (1991).

[11]J. Fejzo, W. M. Westler, J. L. Markley and S. Macura, *J. Am. Chem. Soc.* **114**, 1523 (1992).

[12]C. Zwahlen, S. J. F. Vincent, L. Di Bari, M. H. Levitt and G. Bodenhausen, *J. Am. Chem. Soc.*, in press.

[13]I. Burghardt, R. Konrat and G. Bodenhausen, *Mol. Phys.* **75**, 467 (1992).

[14]A. G. Redfield, *Adv. Magn. Reson.* **1**, 1 (1965).

[15]A. Abragam, "The Principles of Nuclear Magnetism", (Clarendon Press, Oxford, 1961).

[16]A. J. Vega and D. Fiat, *Pure. Appl. Chem.* **40**, 181 (1974);

A. J. Vega and D. Fiat, *J. Magn. Reson.* **13**, 260 (1974);
A. J. Vega and D. Fiat, *J. Chem. Phys.* **60**, 579 (1974);
A. J. Vega and D. Fiat, *J. Magn. Reson.* **19**, 21 (1975).

[17]D. H. Jones, N. D. Kurur and D. P. Weitekamp, *Bull. Magn. Reson.* **14**, 214 (1992).

[18]F. A. L. Anet and D. I. Freedberg, *Chem. Phys. Lett.* **208**, 187 (1993).

[19]L. G. Werbelow and D. M. Grant, *Adv. Magn. Reson.* **9**, 189 (1977).

[20]D. Canet, *Prog. NMR Spectrosc.* **21**, 237 (1989).

[21]J. McConnell, "The theory of NMR Spin Relaxation in Liquids", (Cambridge University Press, Cambridge, 1987).

[22]D. Neuhaus and M. P. Williamson, "The Nuclear Overhauser Effect in Structural & Conformational Analysis", (VCH, Cambridge, 1989).

[23]M. Guéron, J. L. Leroy and R. H. Griffey, *J. Am. Chem. Soc.* **105**, 7262 (1983).

[24]M. Goldman, *J. Magn. Reson.* **60**, 437 (1984).

[25]R. Brüschweiler, C. Griesinger and R. R. Ernst, *J. Am. Chem. Soc.* **111**, 8034 (1989).

[26]R. Brüschweiler and R. R. Ernst, *J. Chem. Phys.* **96**, 1758 (1992).

[27]C. Dalvit and G. Bodenhausen, *Adv. Magn. Reson.* **14**, 1 (1990).

[28]L. Mäler and J. Kowalewski, *Chem. Phys. Lett.* **190**, 241 (1992).

[29]C. Dalvit and G. Bodenhausen, *Chem. Phys. Lett.* **161**, 554 (1989).

[30]M. H. Levitt and R. Freeman, *J. Magn. Reson.* **43**, 502 (1981).

[31]J. S. Waugh, *J. Magn. Reson.* **50**, 30 (1982).

[32]J. S. Waugh, *J. Magn. Reson.* **49**, 517 (1982).

[33]A. J. Shaka and J. Keeler, *Prog. Nucl. Magn. Reson. Spectrosc.* **19**, 47 (1987).

[34]U. Haeberlen and J. S. Waugh, *Phys. Rev.* **175**, 453 (1968).

[35]U. Haeberlen, "High Resolution NMR in Solids. Selective Averaging", (Academic, New York, 1976).

[36]J. Jeener, *Adv. Magn. Reson.* **10**, 1 (1982).

[37]I. Solomon, *Phys. Rev.* **99**, 559 (1955).

[38]R. R. Ernst, G. Bodenhausen and A. Wokaun, "Principles of Nuclear Magnetic Resonance in One and Two Dimensions", (Clarendon Press, Oxford, 1987).

[39]O. W. Sørensen, G. W. Eich, M. H. Levitt, G. Bodenhausen and R. R. Ernst, *Prog. NMR Spectrosc.* **16**, 163 (1983).

[40]V. V. Krishnan and Anil Kumar, *J. Magn. Reson.* **92**, 293 (1991).

[41]Anil Kumar, 5th Chianti Workshop, San Miniato, Italy, May 1993.

[42]L. Di Bari and M. H. Levitt, to be published.

[43]A. G. Palmer III, N. J. Skelton, W. J. Chazin, P. E. Wright and M. Rance, *Mol. Phys.* **75**, 699 (1992).

[44]M. H. Levitt, *Prog. NMR Spectrosc.* **18**, 61 (1986).

[45]L. Di Bari, J. Kowalewski and G. Bodenhausen, *J. Chem. Phys.* **93**, 7698 (1990).

[46]I. Burghardt, Doctoral Thesis, University of Lausanne, 1991.

[47]S. Szymanski, A. M. Gryff-Keller and G. Binsch, *J. Magn. Reson.* **68**, 399 (1986).

[48]M. Ravikumar, R. Shukla and A. A. Bothner-By, *J. Chem. Phys.* **95**, 3092 (1991).

[49]C. Griesinger and R. R. Ernst, *Chem. Phys. Lett.* **152**, 239 (1988).

[50]A lucid description of the rotating frame transformation can be found in Appendix D of J. Jeener and F. Henin, *Phys. Rev. A* **34**, 4897 (1986).

[51]A. G. Redfield, *Phys. Rev.* **98**, 1787 (1955), note 29. In this influential early paper, Redfield indicates that Eqn. 51 is incorrect because "the electrons, which are responsible for the relaxation are almost completely unaffected by the rf field" (p.1796) [this is the case of nuclear relaxation by metallic conduction electrons]. This argument is too weak. A much stronger justification is that $<\mathcal{H}^R_{\rm coh}>$ is not the spin energy, and cannot be used in statistical calculations involving combinations of lattice and spin energies. A truly energetic role of the "rotating-frame Hamiltonian" is inadmissable *in principle*.

[52]B. Boulat and G. Bodenhausen, *J. Chem. Phys.* **97**, 6040 (1992).

[53]G. Strang, "Linear Algebra and its Applications", (Harcourt Brace Jovanovich, San Diego, 1988).

[54]S. Wolfram, "Mathematica: A System for Do-

ing Mathematics by Computer", (Addison-Wesley, New York, 1991).

[55]see ref. (38), p.288.